An Analytical Design Method for Steel-Concrete Hybrid Walls

Peer-reviewed author version

Plumier, André; DRAGAN, Dan; Nguyen, Quang Huy & DEGEE, Herve (2017) An Analytical Design Method for Steel-Concrete Hybrid Walls. In: Structures, 9, p. 185-199.

DOI: 10.1016/j.istruc.2016.12.007
Handle: http://hdl.handle.net/1942/23688

An Analytical Design Method for Steel-Concrete Hybrid Walls

André Plumier, University of Liege, Belgium
E-mail: a.plumier@ulg.ac.be
Address : 36 rue Limoges 4130 Tilff Belgium
André Plumier, University of Liege, Belgium

Dan Dragan, Hasselt University, Belgium
Dan.dragan@uhasselt.be

Nguyen Quang Huy, INSA Rennes, France
Quang-Huy.Nguyen@insa-rennes.fr

Hervé Degée, Hasselt University, Belgium
Herve.degee@uhasselt.be

Abstract

The design of concrete walls or columns reinforced by several encased steel profiles, also called hybrid walls, is similar to the one of classical reinforced concrete, although specific features require adequate design approaches. Experimental research and numerical models demonstrated the feasibility and validity of such structural components, but simple and practical design methods are still lacking regarding their shear resistance. The evaluation of longitudinal shear action effects at the steel profile–concrete interface is a key aspect: research results have been achieved in a more or less recent past for different types of connection but without leading to design conclusions. In this paper, the classical equivalent truss model for reinforced concrete subjected to shear is extended to take into account the contribution of the encased profiles to the shear stiffness and strength. Resulting action effects in the steel profiles, in the concrete and at the steel profile–concrete interfaces are established which allows performing design checks for those three components. In particular, it is evidenced that friction is one of the main component of the resistance to longitudinal shear at the steel profile-concrete interface. It can be directly checked since the proposed method clearly identifies the compression stresses at that location. The validity of the method is assessed by referring to tests results from experimental campaigns in China and in Europe. Some of these tests were carried out without shear connectors welded to the encased steel profiles allowing however achieving the full bending resistance of the element without any apparent problem related to longitudinal shear, like slippage between concrete and steel profile. For some other tests, failure was observed as a consequence of an insufficient shear connection. A detailed assessment of these results shows that the new design proposal is perfectly consistent with all the experimental observations.

Keywords

Composite steel-concrete Walls. Hybrid. Columns. Encased sections. Embedded sections.

An Analytical Design Method for Steel-Concrete Hybrid Walls

1. Introduction

Structural concrete walls are widely used in building structures to provide lateral strength, stiffness, and, in seismic regions, inelastic deformation capacity required to withstand earthquakes. In recent years, steel reinforced concrete (SRC), also called hybrid walls, have gained in popularity. Such walls include steel profiles encased in what for the rest remains a classical reinforced concrete (RC) walls. SRC walls offers the following potential advantages with respect to conventional RC walls: (1) the encased structural steel develops a composite action with concrete, increasing then the compression, bending and shear strength of the walls and reducing the necessary total cross-section area; (2) the steel profiles encased along the wall boundaries increase the deformation capacity and the energy dissipation capacity, these two properties being required for buildings subjected to earthquakes; (3) the encased profiles enhance the weak axis stiffness of the walls and delay the possible out-of-plane buckling failure of wall boundaries; (4) the encased steel profiles can be easily connected with steel and composite steel concrete floor beams that are often used in buildings.

In the past decade, significant experimental research efforts have been devoted to studying the behavior of SRC walls: Wallace et al. [1], Qian et al. [2],Ji et al. [7], Ying et al. [3], Dan et al. [4], [5], [6]. Design provisions for SRC walls have been included in some leading design codes: AISC 341-10 [8], Eurocode 8 [9] and JGJ 3-2010 [10]. Various types of numerical models have also been developed for modeling RC walls: multiple vertical-line-element models, Vulcano et al.[11], Oraksal et al. [12], fiber beam-column models by PEER[13], and multi-layer shear element models: Miao et al.[14] and Lu et al.[15]. However, although all these tests and numerical models do indeed provide valuable knowledge on the behavior of SRC walls, they don't directly lead to practical design tools. Resorting in a systematic way to a validation by testing or by sophisticated FE models requires indeed a huge investment incompatible with the daily practice of design engineers. Sections 2 to 5 propose an analytical method which allows simple and easy design checks for SRC walls subjected to axial force, bending and shear. Sections 6 to 9 present then a validation of the design method by referring to recent experimental tests. These developments were achieved in the frame of the Smartcoco Project funded by the European Commision and dealing with different types of steel-concrete hybrid structures –Degee et al. [16]

2. Analysis and resistance of walls subjected to bending and axial force

In a wall subjected to a combination of design axial force N_{Ed} and bending moment M_{Ed}, encased steel profiles are submitted essentially to longitudinal strains. The contribution of the individual bending stiffness of each profile to the global bending stiffness can be seen as secondary. For instance, in the case of the wall section in figure 1, the stiffness EI_H of the 3 encased HE120B sections is equal to $5.45.10^{12}$ Nmm^2. In comparison, the wall stiffness EI_{wall} calculated for instance according to Eurocode 4 [17] expression is much greater:

$$EI_{eff,II} = 0.45\ E_{cm}I_c + 0.9\ E_sI_s + 0.9E_aI_a = 2,88.10^{14}\ \text{Nmm}^2 \qquad (1)$$

where subscripts a stand for steel profiles and subscript s for classical reinforcing bars.

The ratio EI_H/EI_{wall} is smaller than 2%. This means that the second moment of area of encased steel the profiles, just like the one of classical reinforcement bars, does not significantly contribute to the global wall bending stiffness, so that the section strength in combined bending and compression can be evaluated by common methods used for usual reinforced concrete.

Besides that, it has been shown by Bogdan et al. [19] that the Plastic Distribution Method (PDM), as defined in Eurocode 4 [17] or in AISC2010 [18], and which assumes rectangular stress blocks can also be used.

A subsequent question rises: can a steel profile be reduced to a single bar in the model of the cross-section, or is a group of bars required? The second solution is seen as preferable given that a model with a single bar provides only an approximation of the position of the plastic neutral axis of the wall. The modelling of each steel profile by means of two circular bars for each flange and two for the web -Figure 1- was proved valid by Bogdan et al. [20] who showed that the interaction curves of axial force *N* - bending moment *M* were practically identical for profiles modelled explicitly or by such a set of bars. A modelling with bars was also proved valid for columns with 4 encased profiles.

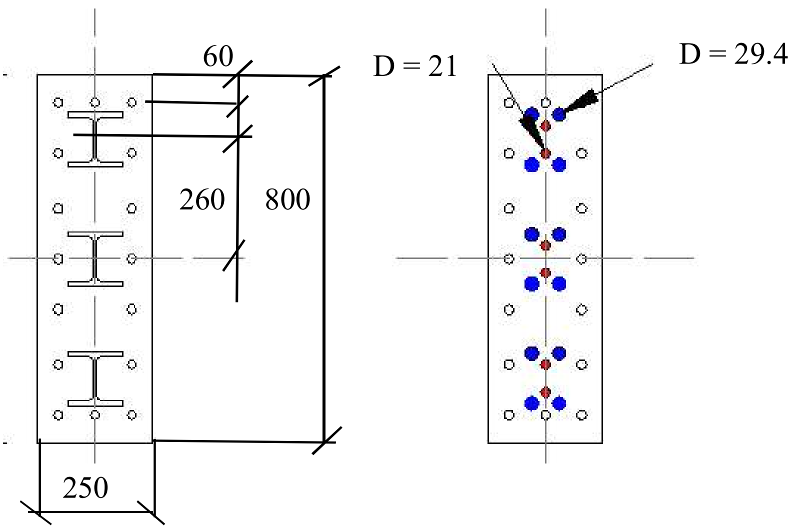

Figure 1 - Wall with 3 encased HEB120 profiles. Left: real section. Right: model with bars diameter D=21mm for the web and D=29.4mm for the flanges. Other characteristics: HEB120 height h = width b = 120mm; flange thickness t_f=11mm; web thickness t_w= 6.5mm. Wall width b_w=250mm. Longitudinal bars diameter: 20 mm. Ratio of cross-sectional area of encased profile to area of boundary zone 250x240mm: 5.7%.

Yield stress and elongation capacity are similar in encased profiles and standard reinforcing bars, but profiles do not present surface indentations. The bond strength of profiles is 7 times lower than the one of ribbed bars and the difference increases for higher concrete classes. It is shown in Plumier et al. [21] that, although profiles exhibit a larger surface to develop the bond, this does not compensate the low bond strength. This results in the fact that a specific design check is required for encased steel profiles, demonstrating that the longitudinal shear between profiles and concrete can effectively be resisted by an adequate shear connection.

Moreover, the effect of the shear force $V_a= V_{a,Ed}$ in each profile on its resistance to axial force has to be considered in the evaluation of the wall resistance to combined bending and axial force, see section 5.

The possibility to define by a straightforward analytical method the transverse shear in each profile as well as the longitudinal shear between steel profiles and concrete corresponding to the applied axial force N_{Ed}, bending moment M_{Ed} and shear $V_{Ed.}$ is thus a need for a practical implementation in the daily design practice.

The classical beam theory was the first reference used to establish a complete calculation procedure for beams subjected to shear – Plumier et al [22]. However, this procedure exhibits two drawbacks. First, the classical beam theory is strictly valid only for elements made of a continuous material resisting equally to tension and compression and not subject to cracking, which is in principle not the case of concrete. Second, the method requires the partition of the wall into subdivisions which are either only reinforced concrete or concrete reinforced by encased profiles. In each subdivision, the calculation of the moment of inertia and of a set of first moment of area corresponding to each plane section where shear is calculated have to be made, so that the calculations become long and tedious.

For those reasons, it was decided to develop an alternative analytical method based on the Mörsch truss model – Mörsch [23], this latter being the internationally recognized reference method in reinforced concrete codes like Eurocode 2 [27] or ACI318-14 [30].

3. Action effects on walls subjected to bending, shear and axial force

3.1 General concept

The total deflection of walls subjected to shear and bending is the sum of a bending component and a shear component, as illustrated in Figure 2:

$$\delta_{tot} = \delta_M + \delta_V \qquad (2)$$

In the truss analogy which is used in reinforced concrete design, bending and shear are taken into consideration in a single truss model in which deformations involve all bars, which all contribute to the truss stiffness by their axial stiffness *EA*. The individual bending and shear stiffness *EI* and *GA* of the bars are neglected. As explained in section 2, this simplification is acceptable for bending stiffness but is questionable for shear stiffness if bars are encased steel profiles: a hybrid wall in which the shear stiffness of concrete would be null keeps the shear stiffness of the encased profiles.

The contribution of encased profiles to shear stiffness can be calculated with the analytical method proposed in 3.2, which is based on the following model and remarks.

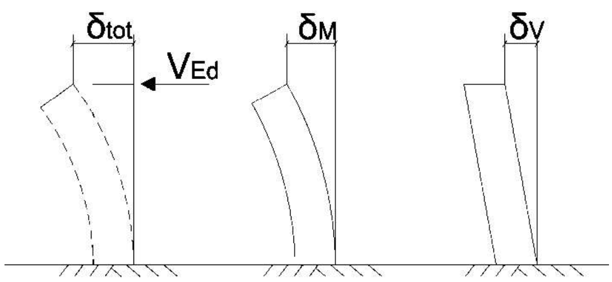

Figure 2. Components of the deformation of walls.

The reference model for shear in reinforced concrete elements is a truss with compression diagonals in concrete and transverse steel ties, while the chords are the truss components designed to resist the bending moment.

In the truss analogy, the model is the same for bending and shear effects, but the respective contributions of shear and bending deformation to the total deformation can be identified.

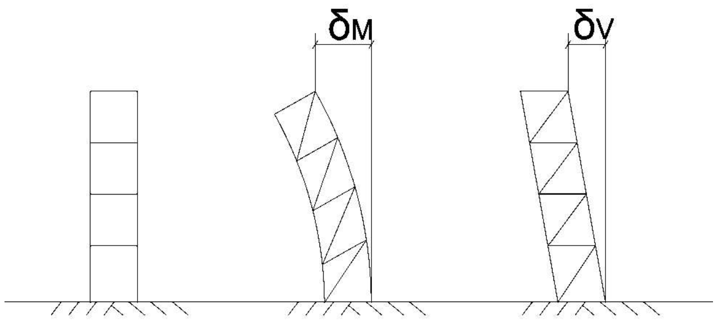

a) Hypothesis 1 b) Hypothesis 2

Figure 3. Deformed shapes of a truss in bending and in shear.

If we consider as Hypothesis 1 a situation where the diagonals and transverse bars are axially infinitely stiff, the horizontal displacement δ at the top of the truss is only due to the axial deformation of the chords. This situation shown in Figure 3a) is equivalent to a “bending flexibility only” situation, parameter EI, and $\delta = \delta_M$.

If we consider as Hypothesis 2 a situation where the chords are axially infinitely stiff, the deformation δ is only due to the axial deformation of the diagonals and transverse bars. This situation shown in Figure 3b) is equivalent to a “shear flexibility only” situation, parameter GA_s, and $\delta = \delta_V$. Axial forces in the bars of the truss are the same for Hypotheses 1 and 2, since the truss system is statically determinate. The encased steel profiles are longitudinal reinforcements which are part of the chords, but we have shown earlier that their own bending stiffness does not influence significantly the bending stiffness of the truss. It results that only the shear stiffness GA_s of the steel profiles has an influence on the shear stiffness of the truss.

A total shear V_{Ed} acting on the truss will be distributed between two shear resisting systems working in parallel and thus proportionally to their relative shear stiffness: V_c into a truss with bars subjected to axial forces and V_a into the set of steel profiles subjected to shear. Figure 4.

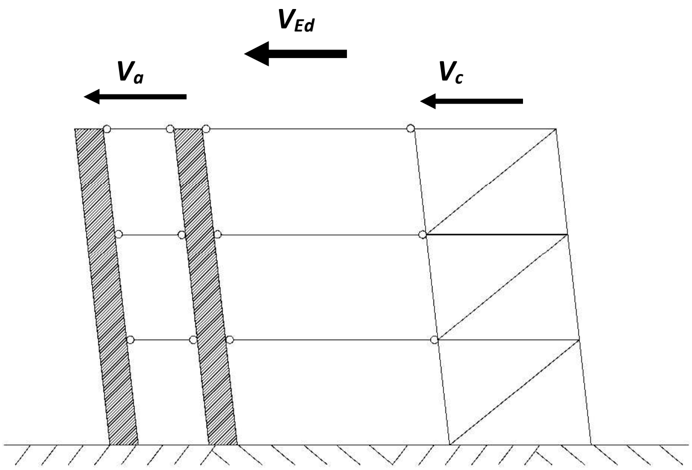

Figure 4. Distribution of the total shear V_{Ed} in two shear resisting systems working in parallel.

3.2 Shear stiffness of the truss

The evaluation is made on a "unit cell" of the truss, z being the distance between the compression and tension chords. In walls with huge encased sections, it is proposed to consider z as the distance between the center of the encased profiles. θ is the inclination of the concrete compression diagonal. The height of the wall corresponding to a "unit cell" is $z\ cot\theta$. For an applied shear V_c, the total horizontal displacement δ_{RC} of the application point of V_c is:

$$\delta_{RC} = \delta_c + \delta_s \tag{3}$$

in which δ_c is the horizontal displacement of the application point of V_c due to the shortening δ_{diag} of the diagonal compression strut and δ_s the horizontal displacement due to the elongation of the stirrups. The elongation of the chord in tension and the shortening of the chord in compression do not influence the horizontal displacement of the application point of V_c. The compression diagonal characteristics are (Figure 5):

$$F_{diag} = V_c / sin\theta \quad (4)$$

$$l_{diag} = z / sin\theta \quad (5)$$

$$b_{diag} = b_w \quad (6)$$

$$h_{diag} = z\ cos\theta \quad (7)$$

$$A_{diag} = b_w h_{diag} = b_w z cos\theta \quad (8)$$

$$E_{diag} = \eta E_c \quad (9)$$

The coefficient η is introduced to take into account the encased profiles which constitute "hard spots" stiffer than concrete in the compression diagonal. The way to calculate η is explained in 3.5.

The displacement δ_c is: $\delta_c = \delta_{diag} \cos\left(\frac{\pi}{2} - \theta\right) = \delta_{diag} \sin\theta = \frac{V_c}{\eta E_c b_w \sin\theta \cos\theta}$ (10)

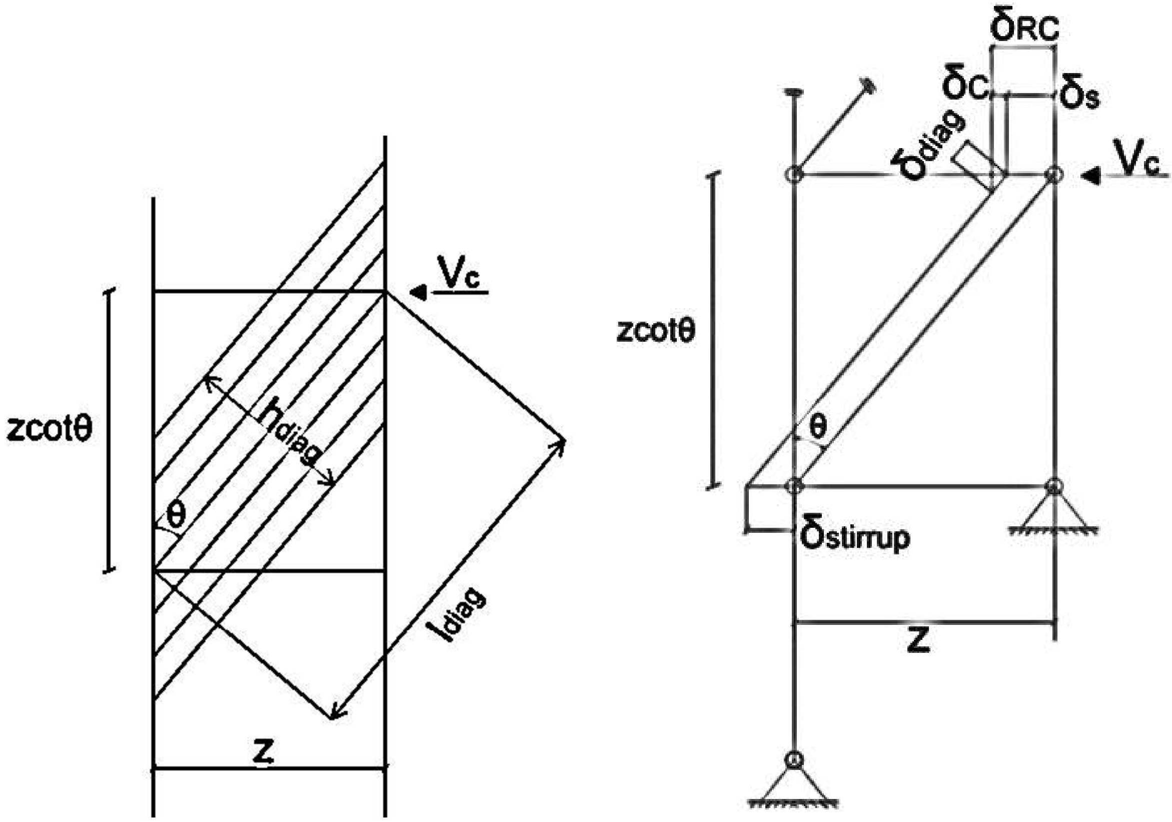

Figure 5. “Unit cell” of Mörsch truss subjected to shear and components of the deformation

The tension force in the stirrups on the unit cell with height $z \cot\theta$ is:

$$F_{stirrups} = V_c \tag{11}$$

A_s is realized by n stirrups with spacing s over the height $z\cot\theta$: $n = z\cot\theta / s$ (12)

$$\delta_{stirrup} = \delta_s = \frac{F_{stirrup} z}{E_s A_s} = \frac{V_c z}{E_s A_s} = \frac{V_c z s}{E_s A_{sw} z \cot\theta} = \frac{V_c s}{E_s A_{sw} \cot\theta} \tag{13}$$

where A_{sw} is the section of one stirrup section (note: it generally means 2 bars]

$$\delta_{RC} = \delta_s + \delta_c = V_c \left(\frac{s}{E_s A_{sw} \cot\theta} + \frac{1}{\eta E_c b_w \sin\theta \cos\theta} \right) \tag{14}$$

The shear stiffness S_{RC} of one “unit cell” of the truss, due to reinforced concrete and stirrups, is:

$$S_{RC} = \frac{1}{\dfrac{s}{E_s A_{sw} \cot\theta} + \dfrac{1}{\eta E_c b_w \sin\theta \cos\theta}} \tag{15}$$

If θ=45°, S_{RC} becomes:

$$S_{RC} = \frac{1}{\dfrac{s}{E_s A_{sw}} + \dfrac{2}{\eta E_c b_w}} \tag{16}$$

3.3 Shear stiffness of the encased steel profiles

The total horizontal displacement δ_{SP} of the application point of the applied shear V_a for a number N of identical encased steel profiles and the shear stiffness S_{SP} for the set of N profiles are established as follows.

$$\gamma = \tau / G = V_a / NGA_v \tag{17}$$

$$\delta_{SP} = \gamma z \cot\theta = (V_a z \cot\theta) / NGA_v \tag{18}$$

$$S_{SP} = (NGA_v) / z \cot\theta \tag{19}$$

If θ=45°, S_{SP} becomes: $S_{SP} = (NGA_v) / z$ (20)

where A_v is the shear area of one steel profile and G is the shear modulus of steel (80769 MPa).

3.4 Distribution of shear between Mörsch truss and the steel profiles

For a total shear V_{Ed} applied to a section of wall with encased steel profile, the total transverse shear V_a applied to the N encased steel profiles is found as:

$$V_a = V_{Ed} S_{SP} / (S_{SP} + S_{RC}) \tag{21}$$

and is supposed equally shared between the N profiles.

The shear applied to Mörsch truss is:

$$V_c = V_{Ed} S_{RC} / (S_{SP} + S_{RC}) \tag{22}$$

3.5 Contribution of encased profiles to the stiffness of the compression diagonal

Encased profiles constitute “hard spots” inside the compression struts (See Figure 6). A part F_a of the inclined compression force F_{diag} goes through the profiles while another part F_c is applied to the concrete around the profile, F_a and F_c being in proportion to the relative stiffness K_a of the profile and K_c of the concrete around the profile. Figure 7.

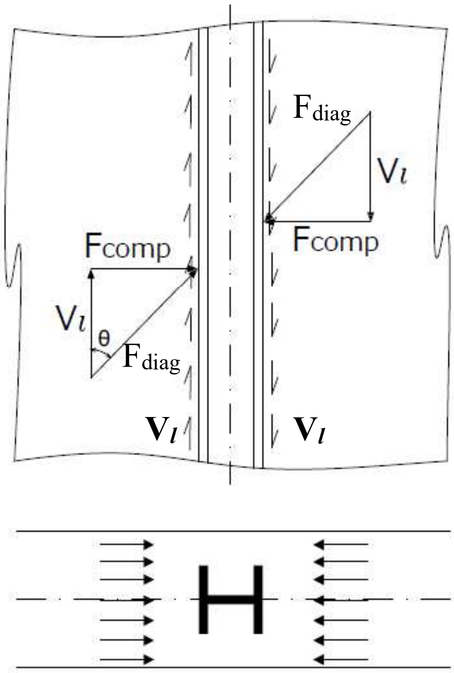

Figure 6. Forces in action at an internal profile.

For the H profile oriented as in Figure 7, the stiffness K_a of the profile, with concrete between flanges included, and K_c of the concrete around the profile are found as:

$$K_c = \frac{E_c \times \left(b_w - b\right)\sin\theta}{h} \tag{23}$$

$$K_a = E_s \sin\theta \Big/ \left[\frac{2t_f}{b} + \frac{h - 2t_f}{\left[t_w + (b - t_w) \times E_c^* / E_s\right]}\right] \tag{24}$$

where E_c^* is a concrete modulus taking into account the effect of confinement.

$\sin\theta$ is due to the fact that the "hard spot" length along the diagonal is $h/\sin\theta$

The reference stiffness of a similar full concrete zone is:

$$K_c^f = \frac{E_c \times b_w \sin\theta}{h} \tag{25}$$

The equivalent modulus E_c^e for the encased profile zone is:

$$E_c^e = \frac{E_c \times (K_a + K_c)}{K_c^f} \tag{26}$$

The coefficient η is then: $\eta = \dfrac{E_c^e \times \left(z - \sum L_i\right) + E_c \times \sum L_i}{zE_c}$ (27)

where L_i represents the distance between the encased profiles – see Figure 8. For example, for the wall of Figure 1 and assuming E_c =30000MPa and E_c^*=45000MPa, η is equal to 1.24

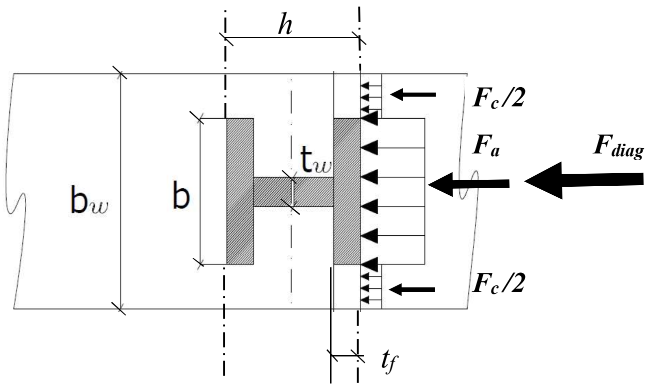

Figure 7. Distribution of F_{diag} into F_a in the profile and F_c in concrete.

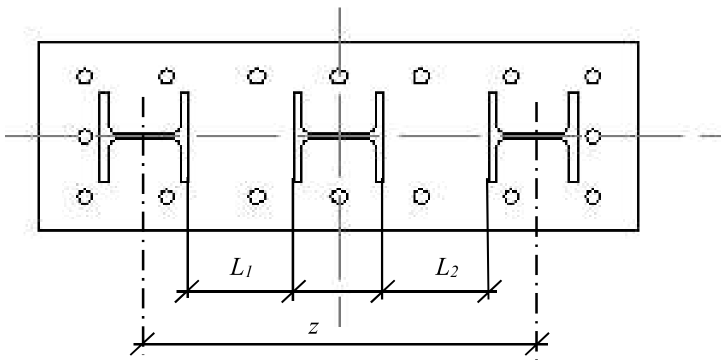

Figure 8. Symbols used in the definition of η

For the H profile oriented as in Figure 9, K_a and K_c are:

$$K_c = \frac{E_c^* \times (b_w - h)\sin\theta}{b} \tag{28}$$

$$K_a = \frac{\left[2t_f E_s + (h - 2t_f)E_c^*\right]\sin\theta}{b} \tag{29}$$

The reference stiffness of a full concrete section without encased profile becomes here:

$$K_c^f = \frac{E_c \times b_w \sin\theta}{b} \tag{30}$$

The coefficient η is then derived as above from eq. (26) and (27). For example, for the wall of Figure 1 and profiles oriented like in Figure 9 and assuming E_c=30000MPa and E_c^*=45000MPa: η is equal to 1.34

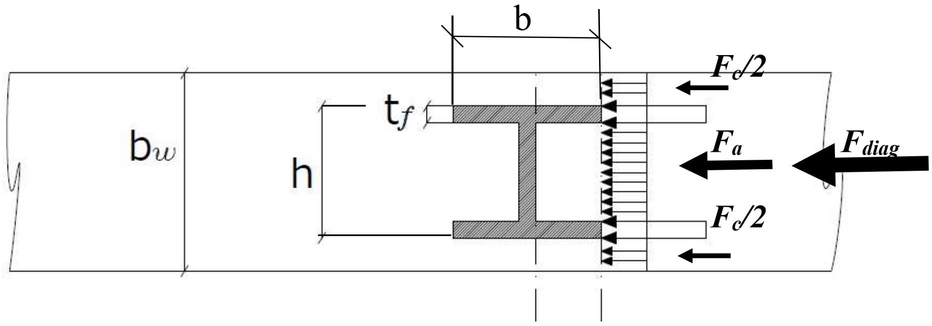

Figure 9. Distribution of F_{diag} into F_a in the profile and F_c in concrete

3.6 Action effects at the interface between concrete and encased profiles

The steel profiles that are present in the chords of the truss model are named here “external” profiles while those not in the chords or boundary zones are named “internal” profiles.

The nodes of the truss model are in the chords; these are the convergence points of the compression strut force F_{diag}, the tie force in the stirrups $F_{stirrup}$ and a vertical force V_l which equilibrates the vertical component of F_{diag}. Figure 10. V_l is induced in the steel components of the chord through longitudinal shear. The horizontal component of F_{diag} is a compression force which equilibrates $F_{stirrup}$. Over a height of wall $z\cot\theta$:

$$V_l = F_{diag}\cos\theta = V_c\cot\theta \tag{31}$$

$$F_{stirrup} = F_{comp} = F_{diag}\sin\theta = V_c \tag{32}$$

$$\text{If } \theta = 45°: \; V_l = V_c \tag{33}$$

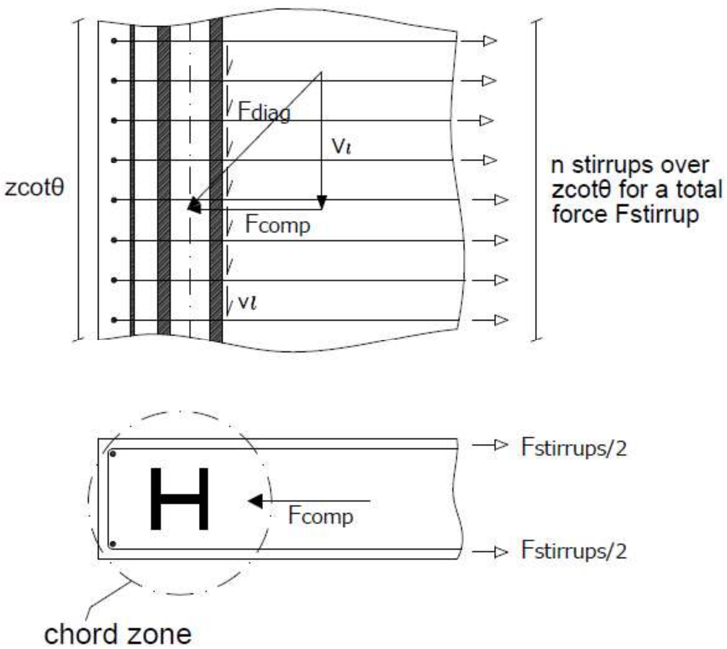

Figure 10. Equilibrium at a node of the truss model.

The chord is constituted of classical bars and of the external steel profile, and the longitudinal shear force V_l is distributed between these components. The shear force applied to the profile is:

$$V_{l,a} = V_l \frac{A_{prof}}{A_{prof} + A_{bars}} \tag{34}$$

where A_{prof} is the profile section and A_{bars} the area of the bars in the chord zone.

For the sake of simplicity and some additional safety, it could be considered in design that:

$V_{l,a} = V_l$ (35)

The distribution of $V_{l,a}$ around the encased profile depends on the general distribution of forces around that profile, which has been related in 3.5 to the relative stiffness K_a of the profile, concrete between flanges included, and K_c of the concrete around the profile. Expressions (36) and (37) can be used to estimate the component $V_{l,a,int}$ which is introduced in the profile on the side facing the concrete compression diagonal and the compoment $V_{l,a,ext}$ which is introduced on the other half of the profile: $V_{l,a,\mathrm{int}} = \dfrac{V_{l,a} K_a}{K_a + K_c}$ (36)

$$V_{l,a,ext} = \frac{V_{l,a} K_c}{K_a + K_c} \quad (37)$$

For example, for the wall of Figure 1 the contributions $V_{l,a,int}$ and $V_{l,a,ext}$ are equal to:

$V_{l,a,int} = 0.66\ V_{l,a}$ and $V_{l,a,ext} = 0.34\ V_{l,a}$.

With the data of Figure 1, but profiles oriented like in figure 9, it yields:

$V_{l,a,int} = 0.55\ V_{l,a}$ $V_{l,a,ext}$=0.45 $V_{l,a}$.

These results indicate that shear connection should be provided on both sides of the external profiles in order to resist the applied longitudinal shear $V_{l,a}$, with 55 to 65% of $V_{l,a}$ to be resisted on the side facing the interior of the wall. The proportion will of course vary, depending on the dimensions of the section and of the encased profiles. Some variability also results from the uncertainty on the modulus E_c* of the confined concrete. In practice, an equal resistance $V_{Rd} \geq V_{l,a,int} = V_{l,a,ext} = 0.5\ V_{l,a}$ can be provided on both sides of the encased profiles.

For a partially encased steel profile in a boundary zone, like the example in figure 10, the applied longitudinal shear is 100%$V_{l,a}$ on the side of the profile facing the diagonal compression strut.

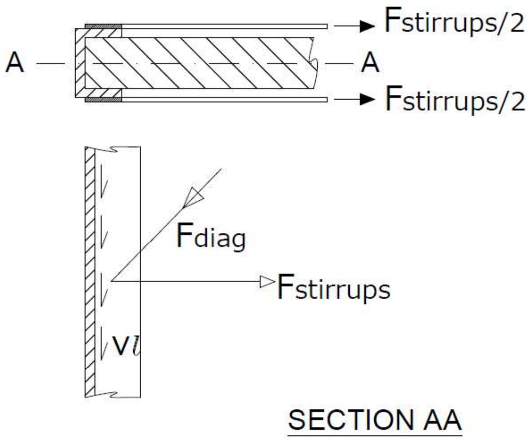

Figure 11. Node equilibrium in case of a partially encased steel profile and external ties

Internal profiles do not participate to the Mörsch truss but the inclined diagonal compression force has to go through the profiles-see Figure 6. A longitudinal shear $V_{l,a}$ is applied on each side of the profile and resistance to $V_{l,a}$ has also to be provided on both sides of each internal profile.

4. Resistance to longitudinal shear at steel-concrete interface

4.1 Resistance to longitudinal shear at steel concrete interface in the context of Eurocode 4

Resistance $V_{l,Rd}$ to an applied longitudinal shear $V_{l,a}$ can be provided by bond, friction and shear connectors, appropriate partial safety factors being considered. The design check in external profiles and internal profiles should be respectively:

$$V_{l,a} \leq V_{l,Rd} \quad (40)$$

$$2V_{l,a} \leq V_{l,Rd} \quad (41)$$

Eurocode 4 allows to sum up the bond, friction and shear connectors contributions in order to obtain the necessary total resistance $V_{l,Rd}$:

$$V_{l,Rd,total,} = V_{Rd,bond} + V_{Rd,friction} + V_{Rd,connectors} \qquad (42)$$

Bond strength $V_{Rd,bond}$ can be calculated with the design shear strength τ_{Rd} defined in Table 6.6 of Eurocode 4, amplified by a factor β greater than 1.0 if the concrete cover is greater than 40 mm. $V_{Rd,bond}$ is the product of τ_{Rd} by an area equal to the product of the height $z\cot\theta$ of steel profile by half the perimeter of the steel profile times β in internal profiles and by the complete perimeter in external profiles.

Friction strength $V_{Rd,friction}$ can be calculated with a μ friction coefficient equal to 0.5 (for steel without painting). Friction results from the compression forces F_a which are part of the compression strut force F_{comp} explained in 4.:

$$V_{Rd,friction} = 0.5\, F_a \qquad (43)$$

Local compression struts at shear connectors welded on the web of an H section can provide an additional friction strength which may be assumed equal to $\mu P_{Rd}/2$ on each flange and for each horizontal row of studs if the conditions defined in figure 12 are respected. P_{Rd} is the design value of the shear resistance of a single connector.

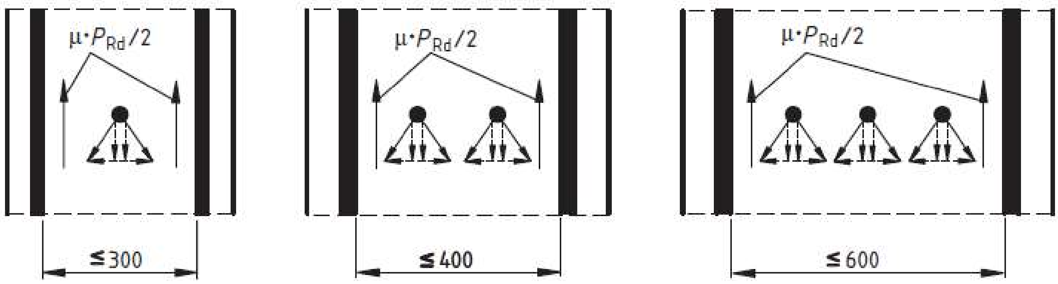

Figure 12. Additional frictional forces $\mu P_{Rd}/2$ in composite columns by use of headed studs (Eurocode 4 Figure 6.21)

A resistance $V_{Rd,connectors}$ to longitudinal shear can also be provided by connectors, headed studs, welded plates or other. With headed studs, if the distance from the wall or column surface to the connector is less than 300 mm, measures should be taken to prevent longitudinal splitting.

With welded plates, measures should be taken to prevent spalling of the concrete if the compression struts developed at the connector is directly facing a wall face: stirrups or links designed to resist a tension force equal to the shear capacity of the connector should be placed at each connector. Plates welded on an encased profile, like in Figure 13, can achieve a direct bearing for the concrete compression struts and provide resistance to longitudinal shear. They can be designed by a "strut and tie" method. In the case of Figure 13, the resistance to longitudinal shear V_{Rd} is equal to:

$$V_{Rd} = ab^{*}\sigma_{c,Rd,max} \qquad (44)$$

where a is the width of the plate: a=(b-2t_w)/2 and b^* is the length of the plate: $b^*=h-2t_f$

$\sigma_{c,Rd,max}$ is the concrete strength in a compression strut:

$$\sigma_{c,Rd,max} = 0{,}6\, v' f_{cd} \qquad (45)$$

with $v'=1-f_{ck}/250$ (46)

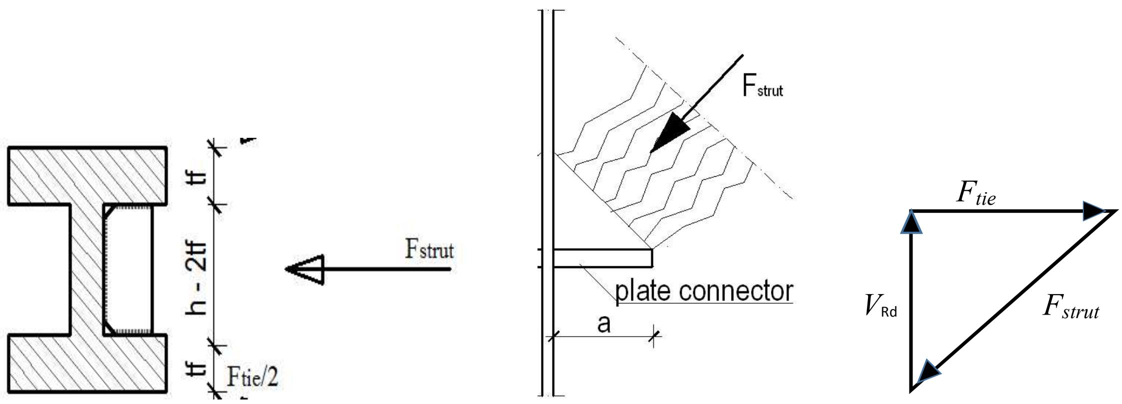

Figure 13. Strut and tie model to determine the welded plate connector strength

4.2 Consistency of longitudinal shear V_l found by beam theory and by truss model.

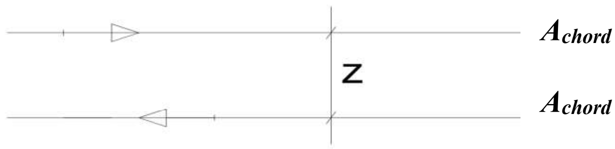

Figure 14. Model considered to apply the theory of beams

The beam theory applied under the hypothesis that the beam consists of two flanges of area A_{chord} with a web considered as a plate with a negligible contribution to inertia I defines a longitudinal shear V_l at the chord:

$$V_l = V_c \, S \, z \, / \, I \qquad (47)$$

where z is the lever arm of internal forces, S the first moment of area of a chord ($S=A_{chord}\, z/2$) and I the second moment of area of the beam ($I=2A_{chord}\,(z/2)^2$).

It results that $V_l = V_c$

which is identical to (26) obtained with the truss model for $\theta = 45°$.

5. Resistance of walls to transverse shear

In a wall subjected to combined compression N_{Ed}, bending moment M_{Ed} and shear V_{Ed}, the design checks should be carried out as follows.

Under combined compression N_{Ed} and bending moment M_{Ed} , the encased steel profiles are simply additional longitudinal reinforcements which participate to the resistance (see 3.) and the reinforced concrete section should be checked accordingly.

With an applied shear force V_c defined by (8), classical checks of reinforced concrete should be used. In the context of Eurocode 2, the most restrictive of the ultimate limit state $V_{Rd,max}$ corresponding to concrete compression struts crushing or $V_{Rd,s}$ corresponding to yielding of the transverse reinforcement governs the design. If $V_{Rd,max} > V_{Rd,s}$, the ultimate limit state of the RC wall in shear corresponds to yielding of transverse reinforcement, which, like yielding in shear of the steel profiles, is a plastic mechanism. In that case, the maximum shear resistance of a wall with encased profiles can be estimated as the addition of the resistance of reinforced concrete corresponding to the yielding of stirrups to the resistance of the steel profiles in shear $V_{Rd,a}$:

$$V_{Rd} = V_{Rd,s} + V_{pl,Rd,tot} \tag{48}$$

where $V_{pl,Rd,tot}$ is the sum of the shear resistance of the encased profiles.

Due to their stiffness in shear, the steel profiles attract a part of the shear and are thus subjected to a combination of axial and shear stresses. The steel profiles should then be checked in axial tension or compression (resulting from bending M_{Ed} + axial force N_{Ed}) combined to shear V_a defined by (7). Shear can reduce the tension or compression resistance of the profile. The corresponding rule in Eurocode 3 is that the effect of shear on tension/compression resistance is negligible if the calculated shear $V_{a,i}$ in one profile i complies with:

$$V_{a,i} \leq 0{,}5\ V_{pl,Rd}. \tag{49}$$

If the calculated shear $V_{a,i}$ in one profile is such that: $0{,}5\ V_{pl,Rd} < V_{a,i} \leq V_{pl,Rd}$,

the tension or compression resistance of the shear area A_v of the steel profile reduces to:

$$(1\text{-}\rho)A_v f_{yd} \tag{50}$$

where $\rho = (2V_{a,Ed}/V_{pl,Rd} - 1)^2$ (51)

Such a loss is likely to affect the profiles in the boundary zones, but normally not the internal profiles.

6. Assessment of the proposed analytical method

6.1 Specific features of the reference experiments

The assessment of the proposed analytical method resorts to results from experimental tests by Qian[2], Dragan [25] and Huy [26], specifically selected because of the following interesting features.

In the tests presented in Qian[2], no shear connectors are present on the encased steel profiles and the ultimate bending moment is achieved without any problem related to longitudinal shear between concrete and steel profiles.

In the tests of the Smartcoco Project [2] [25] [26], 12 walls have been tested. They are characterized by the same dimensions and encased profiles, with some tests including shear connectors and other not. Different types of connectors and different orientation of the encased H sections are also tested. The high steel profile content of the Smartcoco specimens provides useful information for the practice since one of the main aims of hybrid walls is a reduction of the walls dimensions in plan.

6.2 Definitions of parameters used to characterize the test specimens

Besides geometrical data, the main parameters used to characterize the tested specimens are the steel profile content ρ_a, the total steel content $\rho_{s,tot}$, the mechanical ratio δ of Eurocode 4 [17] and the plastic resistance to compression $N_{\mathrm{pl,Rd}}$ of Eurocode 4:

$$\rho_a = A_a / A_c \tag{52}$$

$$\rho_{s,tot}=(A_a+A_s)/A_c \tag{53}$$

$$\delta=A_a f_{\mathrm{yd}}/N_{\mathrm{pl,Rd}} \tag{54}$$

$$N_{\mathrm{pl,Rd}}=A_a f_{\mathrm{yd}}+0.85A_c f_{\mathrm{cd}}+A_s f_{\mathrm{sd}} \tag{55}$$

where A_c is the gross area of concrete and A_a the total area of steel profiles.

A_s is the total area of re-bars in the section.

f_{yd} is the yield stress of the steel profiles

f_{sd} is the yield stress of the reinforcing bars.

A difficulty in the comparisons comes from to the variability of the resistance to longitudinal shear. Eurocode 4 [17] indicates a design shear strength τ_{Rd}=0.3 MPa for concrete encased steel sections and a friction coefficient μ=0.5 at concrete-steel profile interface, while τ_{Rd} measured in tests can be significantly greater. Push out tests of steel profiles in Degee et al.[16] showed values of τ_{Rd} above 0.9MPa. Bond strength and friction coefficient μ depend actually strongly on the surface state and are characterized by a large scatter. In the following, the assessment of design situations is made based on the Eurocode 4 design values: τ_{Rd} =0.3 MPa and μ=0.5. For the comparison of calculation results to experimental results, probable average values of τ_R and μ are selected: $\tau_{R=}$0.6MPa and μ=0.6.

7 Assessment of the analytical method on tests at University of Liege. Dragan et al. [25]

7.1 Test specimens, testing conditions and global results.

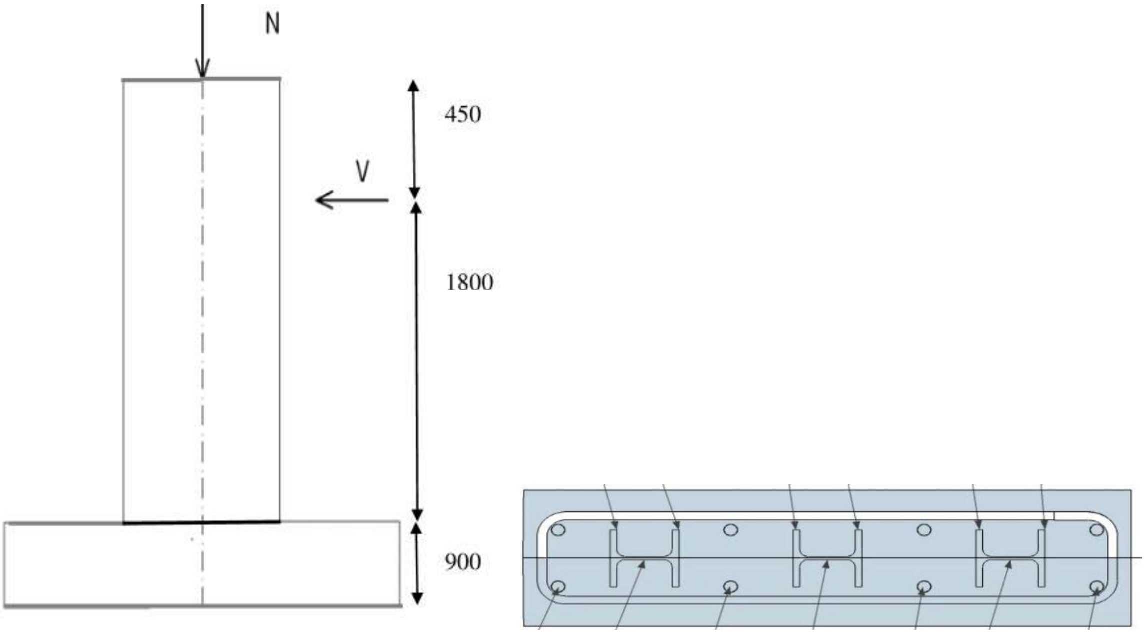

Figure 15. Test configuration. Wall section and position of the strain gages and rosettes

The specimens are cantilever walls. Specimen ARC is a reference reinforced concrete specimen with the same bars as the composite walls BS, CS, CSN, DS and DSN. Specimens ARC, BS, CS, DS are tested in pure bending under a static horizontal load V. Figure 15. Specimens CSN and DSN are additionally subjected to a constant axial force N=1000 kN. The characteristics of the specimens are shown in Figure 16. All wall sections are: b_w x h = 240 x 880 mm. The shear span ratio, or aspect ratio, of the tested walls is equal to λ_R=$H/2h$=1800/880=2.05 with H measured from the basis to the level of horizontal load application axis. The total height of the walls is 2250 mm. All specimens comprise 3 encased steel profiles HEB100 class S460 with web parallel to the wall faces. No shear connectors are present in specimen BS. Headed studs are present in specimens CS and CSN. Plate connectors are installed in specimens DS and DSN. The total shear area of three steel profiles is A_v = 904 x 3 = 2712 mm². Stirrups are at 100mm step s. The longitudinal reinforcement ratio ρ_s is 1.19 %. The total reinforcement ratio $\rho_{s,tot}$ is 3.5%. The mechanical ratio δ (eq.(54)) is equal to 0.41. The concrete characteristic strength established by tests on cylinders is f_{ck} = 55 MPa. Steel profiles have a perimeter of 536mm. Reinforcement are made of S500 steel.

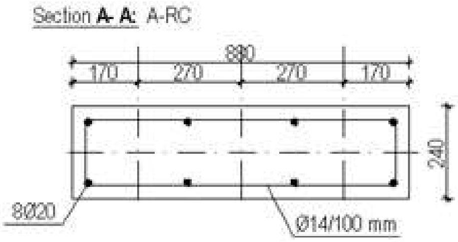

Specimen ARC. Cross-sections

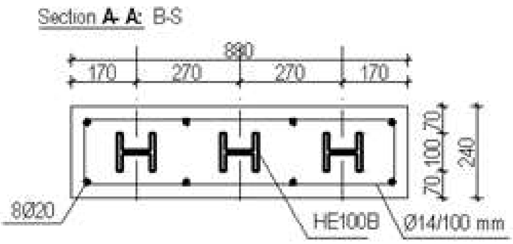

Specimen BS cross-section

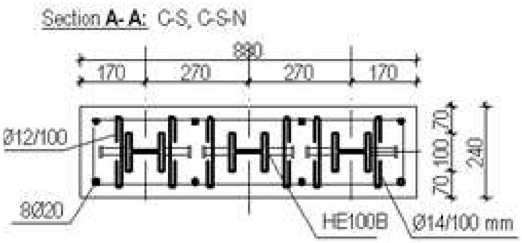

Specimen CS and CSN cross-sections

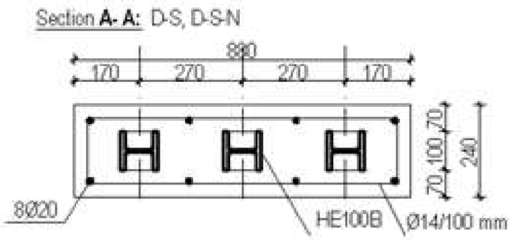

Specimen DS and DSN cross-sections

Figure 16. Sections of Smartcoco D6-2 specimens [5]

Figure 17 shows Horizontal Force – Displacement diagrams at the load application level. The reference reinforced concrete specimen ARC and, amongst the SRC specimens, CS and CSN with headed studs connectors behaved in a ductile way and reached plastic bending. Specimens with plate connectors suffered early failure due to a lack of transverse stirrups supporting the compression struts from each plate connector; this was expected, but nevertheless tested to confirm that design guidance should require these local stirrups.

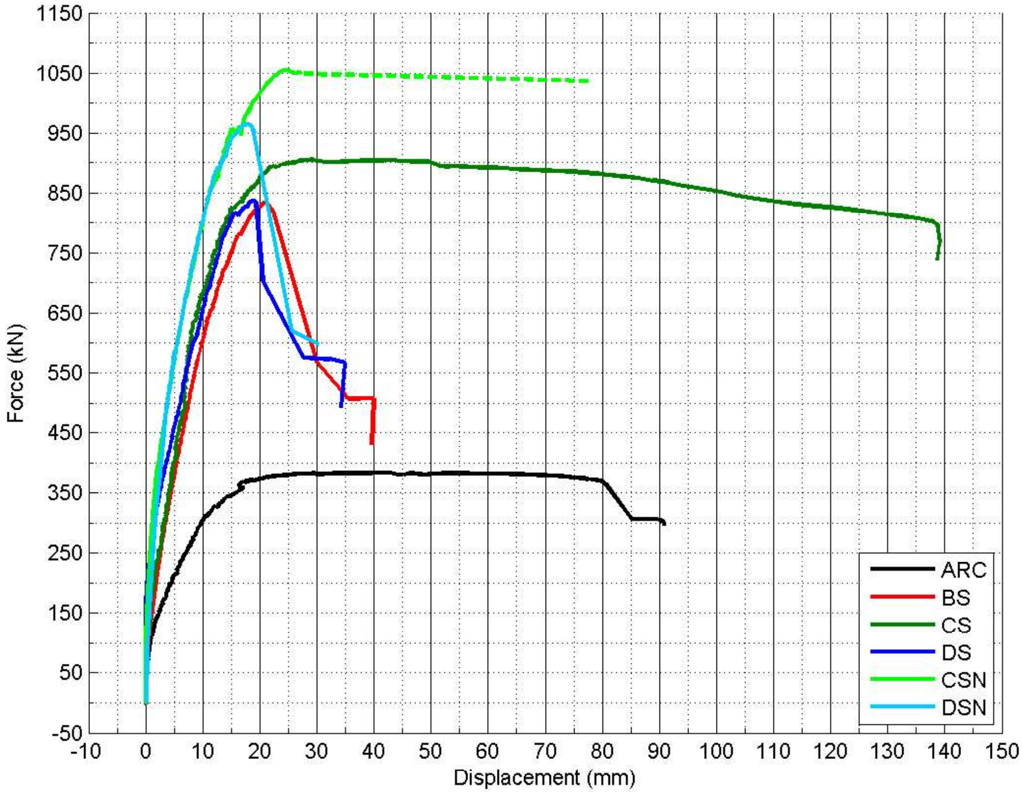

Figure 17. Horizontal Load-Horizontal Displacement diagram

7.2 Resistance of walls to transverse shear

The following parameters are used in the calculations: z= 540 mm, E_c=33000 MPa, E_c^*=49500MPa and η=1.17. Expressions (15), (16), (19) and (21) are used to obtain the results of Table 1 with three hypotheses on θ: θ=45°, 40° and 30°.

All Specimens	Shear stiffness S_{RC} (N/mm)	Shear stiffness S_{SP} (N/mm)	$\frac{S_{RC}}{S_{RC}+S_{SP}}$	$\frac{S_{SP}}{S_{RC}+S_{SP}}$	Resultant calculated shear V_a in profiles at V_{Ed} = 600 kN (kN)
θ = 45°	568.10^3	406.10^3	0.58	0.42	252
θ = 40°	659.10^3	340.10^3	0.66	0.34	204
θ = 30°	875.10^3	234.10^3	0.79	0.21	126

Table 1. Calculated distribution of shear between *RC* truss and steel profiles *SP*.

A comparison of calculated and measured resultant shear forces in steel profiles is made at V_{Ed} = 600 kN (load level lower than the yield load, see Table 2). The shear stresses are measured by means of 9 strain rosettes placed on the steel profiles web at 0 mm, 270 mm and 540 mm from the wall base. The 90° rosettes are glued on the profiles and protected against moisture before pouring concrete. The maximum and minimum principal stresses and the maximum shearing stress τ_{max} at a rosette are deduced from the 3 strain measurements according to a processing which can be found in TML [28]. The shear force V_a is found for each profile as:

$$V_a = A_v \times \tau_{max} \tag{56}$$

where A_v is the shear area of the profile defined in Eurocode 3[29], herein roughly equal to the web area.

The measured shear is different in the 3 encased profiles for one given specimen. There is however some regularity in the total of the shear measured in the three profiles, except with specimens DS and DSN in which the measures at rosettes may have been influenced by the plate connectors reaction to compression struts. In specimens BS, CS and CSN, the agreement between measured to calculated shear in profiles is acceptable and safe-sided for θ=40°, with "calculated vs. measured" ratios ranging from 1.58 to 1.00 with an average equal to 1.17.

Specimen	Level Of Gages	Measured Total Shear in profiles kN	Calculation / Measured At θ=45°	Calculation / Measured At θ=40°	Calculation / Measured At θ=30°
BS	1	162	1.52	1.22	0.74
	2	148	1.66	1.34	0.81
	3	125	1.97	1.58	0.96
CS	1	201	1.22	1.01	0.59
	2	191	1.29	1.03	0.63
	3	192	1.28	1.03	0.63
CSN	1	X	X	X	X
	2	169	1.46	1.17	0.71
	3	199	1.23	1.00	0.60
DS	1	192	1.28	1.03	0.63
	2	137	1.79	1.44	0.88
	3	132	1.86	1.50	0.91

DSN	1	X	X	X	X
	2	114	2.15	1.73	1.05
	3	87	2.82	2.27	1.37

Table 2. Total shear of 3 steel profiles at V_{Ed}= 600 kN. Comparison to calculation results.

Shear in the steel profiles is low and does not reduce the capacity of the profiles in tension:

V_a = 369 kN at V_E =900 kN $\quad$ $V_{pl,Rd}$=(460 x 904 x 3)/√3 = 720 kN

$V_a/V_{pl,Rd}$ = 0.51 $\quad$ ρ= (2 x 369/720 – 1)^2 = 0.0006

The RC walls resistance to shear is calculated with the effective material strength.

Concrete compression struts failure: $V_{Rd,max}$ = 240 x 540 x 0,6 x 55 = 4276kN

Yielding of transverse steel: $V_{Rd,s}$ = 308 x 540 x 500 / 100 = 832 kN

Yielding of 3 steel profiles in shear: $V_{Rd,a}$ = 3 x 904 x 460 / √3 = 720 kN

The maximum applied load is V_{Ed}=1050kN in specimens CS and CSN. This gives the contribution of steel profiles to global shear resistance, since the RC wall resistance is $V_{Rd,s}$=832 kN .

The maximum V_{Ed} in tests is lower than the theoretical maximum resistance $V_{pl,Rd}$ + $V_{Rd,s}$ (1552kN) since other ultimate limit states are reached for lower load levels: specimens CS and CSN fail in plastic bending for V_{Ed} = 1050 kN; specimen BS (without connector) exhibits a bond + friction failure for V_{Ed} = 830 kN; and specimens DS fail in shear at V_{Ed} = 830 kN due to a lack of stirrups.

7.3 Longitudinal shear at concrete-profile interface.

The evaluation of longitudinal shear is made for a transverse shear force V_{Ed} equal to the maximal horizontal load, V_{Ed} = 900 kN (specimen CS), which corresponds to full plastic bending of the wall. θ=40° is considered for the compression struts and $V_{l,a}$ is calculated considering (31) and (34) with A_{bars} of 2 diameter 20 and A_{prof} of one HEB100 in the chord zone.

The results given in Table 3 show that in the framework of a design procedure (1st line in Table 3), shear connectors are required to provide at least a shear resistance of (564 – 384) = 180kN over the "unit cell" height. The transverse shear force failure V_{Ed} corresponding to the estimated failure of specimen BS is equal to 900 x 525 / 564 = 838 kN, which represents a good estimate of the actual failure load of the specimen BS (830 kN).

Specimen BS	V_{Ed} (kN)	V_a (kN)	V_c (kN)	$V_{l,a}$ (kN)	$V_{Rd,bond}$* (kN)	$V_{Rd,friction}$ (kN)	$V_{Rd,total} \Leftrightarrow V_{l,a}$ (kN)
With design parameters	900	306	594	564	82	302	384 < 564
With average parameters	900	306	594	564	163	362	525 < 564

*$V_{Rd,bond}$ includes the β factor of Eurocode 4 for concrete cover greater than 40mm; here β=1,6

Table 3. Applied and resistant longitudinal shear in specimen BS (no shear connectors).

8 Assessment of the analytical method on tests at INSA Rennes [26]

8.1 Test specimens, testing conditions and global results

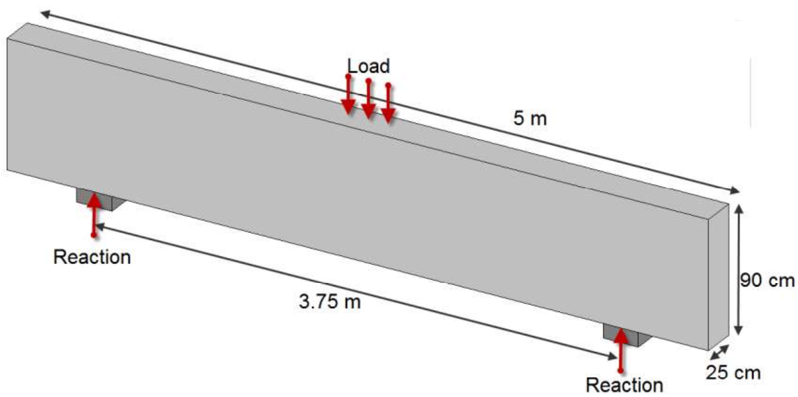

Figure 18. Smartcoco D6-1 test configuration

A 3-point bending test configuration is used to evaluate the resistance of walls to combined bending and shear without axial force. See Figure 18. The specimens are shown in Figure 19. The wall sections are b_w x h = 250 x 900 mm². The shear-span ratio, encased profiles sections, yield stress and longitudinal reinforcement ratios are the same as for the specimens tested at the University of Liege, described in 7. The profiles flanges are parallel to the wall faces so that the total shear area of three steel profiles is equal to A_v = 6360 mm². No shear connectors are present in specimen BW. Diameter 16mm headed studs are used in specimens CW and CWHC with a spacing of 200mm. Plate stiffeners 80 x 40 x 10mm are used as connectors in specimens DW and DWHC with a spacing of 200mm. The stirrups are made of diameter 14mm S500 bars (actual yield stress 633 Mpa) with a spacing of 200mm in specimens ARC, BW, CW and DW (shear reinforcement ratio ρ_w=0.62 %) and with a spacing of 100mm in specimens BWHC, CWHC and DWHC (ρ_w=1.23 %). Concrete strength on cylinders at the test day is 32 MPa, except for specimen BWHC (26 MPa).

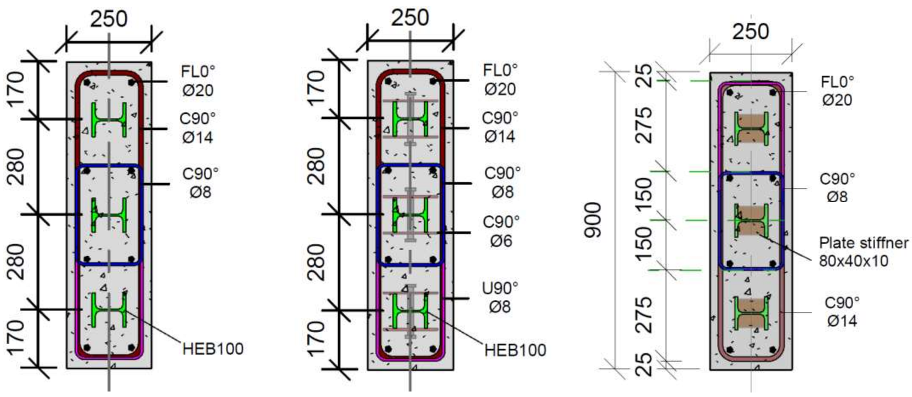

Specimens BW & BWHC CW & CWHC DW & DWHC

Figure 19. Sections of the specimens. Unit: mm.

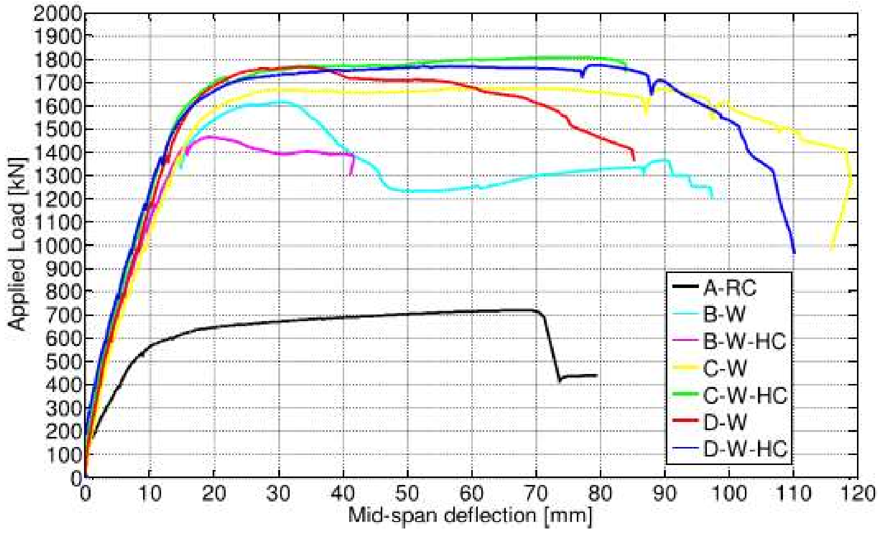

Figure 20. Experimental load displacement curves (note: Applied Shear V_{Ed} = 0.5 Applied Load).

8.2 Resistance of walls to transverse shear

The assessment of the shear force acting on the steel profiles is carried out for the maximum total transverse shear force V_{Ed} reached for each test. Figure 20 and Table 5. The parameters used in the calculations are: z=560 mm, θ=45°, E_c=33000 MPa and η=1.16. Expressions (15), (16), (19) and (21) are used to obtain the results of Table 4. The shear resistance of the walls calculated with the actual material strength are given in Table 5.

Specimens	Shear stiffness S_{RC} (10^3 N/mm)	Shear stiffness S_{SP} (10^3 N/mm)	$\frac{S_{RC}}{S_{RC}+S_{SP}}$	$\frac{S_{SP}}{S_{RC}+S_{SP}}$	Resultant calculated shear V_a in profiles at V_{Ed}=600kN (kN)
BW – CW - DW	303	917	0.25	0.75	450
BWHC – CWHC-DWHC	569	917	0.38	0.62	372

Table 4. Calculated distribution of shear in *RC* truss and steel profiles *SP*.

Specimen	V_{Ed} (kN)	$V_{Ed,max}$ (kN)	$V_{Rd,s}$ (kN)	$V_{pl,Rd,tot}$ (kN)	$V_{pl,Rd,tot}+V_{Rd,s}$ (kN)	$\frac{V_{pl,Rd,tot}+V_{Rd,s}}{V_{Rd,s}}$		V_c kN	$\frac{V_{Ed,s}}{}$

						V_{Ed}	V_{Ed}		V_c
BW	807	1914	790	1069	1859	2.30	0.98	194	4.07
BWHC	725	1922	1580	1069	2649	3.60	2.17	275	5,72
CW	840	1944	790	1069	1859	2.22	0.94	202	3.91
CWHC	905	1922	1580	1069	2649	2.93	1.75	344	4.59
DW	884	1988	790	1069	1859	2.10	0.89	212	3.72
DWHC	887	1901	1580	1069	2649	2.99	1.78	337	4.68

Table 5. Shear resistance of the RC walls

It can be seen in Table 5 that, without the contribution $V_{pl,Rd,tot}$ of the steel profiles to the total shear resistance, the specimens BW, CW and DW would have failed in shear by yielding of stirrups, since $V_{Rd,s}$ is smaller than V_{Ed}. Moreover, since ($V_{pl,Rd,tot} + V_{Rd,s}$) is much greater than V_{Ed}, the observed ultimate limit state is a ductile bending.

In order to assess the evaluation of the shear force V_a in the steel profiles obtained by using the analytical model, a value of the total acting shear force equal to V_{Ed}=600kN is considered, namely a lower load level than the yield load of the walls in plastic bending (note: V_{Ed}=600kN correspond to a total applied load of 1200 kN in Figure 20). Experimental values of the shear force in the steel profiles is established from measurements by rosettes on the flanges. The central line of rosettes R2-R5-R8 (see Figure 21) is located at a distance greater than the section height both from the load introduction point and from the supports and can therefore be considered as not influenced by local disturbances. This line is thus selected for further comparison.

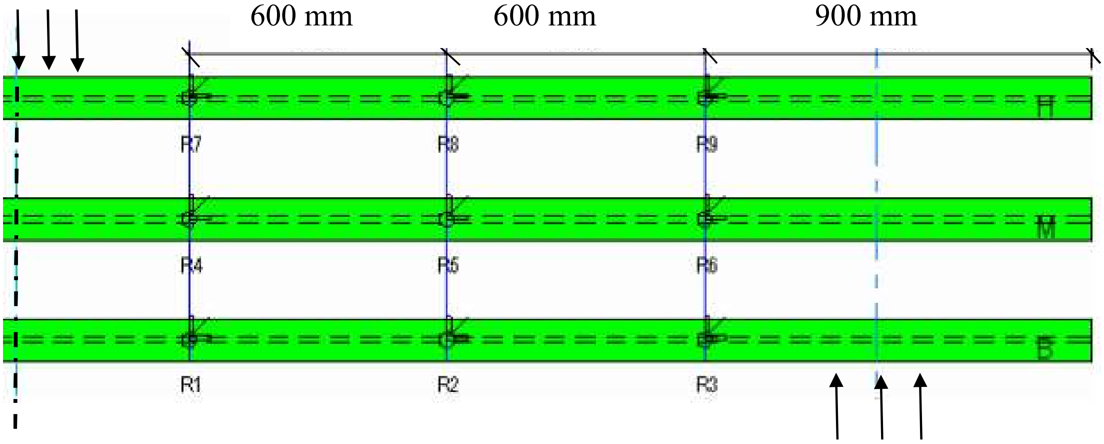

Figure 21. Position of the rosettes.

Specimen	Shear force rosette R2 (kN)	Shear force rosette R5 (kN)	Shear force rosette R8 (kN)	Measured Total Shear In profiles (kN)	Calculated Total Shear In profiles (kN)	Ratio $\frac{\text{Calculation}}{\text{Measured}}$
BW	129	40	64	493	450	0.91
BWHC	105	48	32	392	372	0.95
DW	129	32	64	477	450	0.94

Note: due to deficient rosettes, CW, CWHC and DWHC do not provide comparable data.

Table 6. Comparison of measured and calculated shear in profiles at V_{Ed} = 600 kN

It can be noticed that, in all specimens, the measured shear forces are different for the 3 encased profiles, though there is a regularity in the difference, the lower profile of Figure 21 being systematically more stressed. The sum of the individual shear measured in each profile fits well with the theoretical predictions, with calculation/measurement ratios ranging from 0.93 to 0.96. Shear in the profiles remains low enough not to reduce the capacity in tension. At most, at V_{Ed}=900 kN, $V_a/V_{pl,Rd,tot}$ is equal to 684/1689 = 0.40 < 0.50 so that interaction between axial force and shear in the profile can be neglected -Eurocode 3[29].

8.3 Assessment of expressions for longitudinal shear at concrete-steel profiles interface.

The evaluation is made for a transverse shear force V_{Ed} equal to the maximum load in each test. θ=45° is considered for the compression struts and $V_{l,a}$ is calculated using (31) and (34) with A_{bars} of 2 diameter 20 and A_{prof} of one HEB100 in the chord zone.

	Spec.	V_{Ed} (kN)	$\frac{S_{RC}}{S_{SP}+S_{RC}}$	V_a (kN)	V_c (kN)	$V_{l,a}$ (kN)	$V_{Rd,bond}$* (kN)	$V_{Rd,friction}$ (kN)	$V_{Rd,total} \Leftrightarrow V_{l,a}$ (kN)
1	BW	807	0.25	605	202	181	73	87	160 < 181
2	BWHC	725	0.38	450	275	256	73	124	197 < 256
3	CW	840	0.25	605	235	188	73	91	164 < 188
4	CWHC	905	0.38	561	344	321	73	155	236 < 321
5	DW	884	0.25	663	221	198	73	95	168 < 198
6	BW	807	0.25	605	202	181	86	116	202 > 181
7	BWHC	725	0.38	450	275	257	86	165	251 < 257

*$V_{Rd,bond}$ including β factor of Eurocode 4 for concrete cover greater than 40mm; here β=1,7

Table 7. Evaluation of applied longitudinal shear V_l and comparison to the design resistance to longitudinal shear $V_{Rd,total}$ provided by bond and friction calculated with design values (lines 1 to 5) and calculated with average experimental values (lines 6 and 7) .

The main observations are as follows:

For design conditions, V_{Rd} is lower than $V_{l,a}$ in all specimens and shear connectors are required to provide at least a shear resistance equal to [$V_{l,a}$ - V_{Rd}] kN over the "unit cell" height. This corresponds to the experimental observation: specimens without connectors did not reach an ultimate state in bending.

The transverse shear force V_{Ed} corresponding to a longitudinal shear failure at concrete-steel profiles interface in specimen without connectors is correctly estimated by the proposed method as far as the most likely values of bond and friction parameters are taken into consideration, i.e. 202kN≈181kN for specimen BW and 251kN≈257kN for specimen BWHC (see Table 7 last two lines).

9 Assessment of the analytical method based on tests at Tsinghua University [2]

9.1 Test specimens, testing conditions and global results

In this test series, no shear connectors are placed on the encased CHS steel profiles and, in spite of this, the full ultimate bending moment is achieved without problem related to longitudinal shear, such as slippage between concrete and steel profile. The characteristics of specimens SW2 to SW6 are given in figure 22. Wall sections are h x b_w = 1300 x 160 mm, with a wall height H=2600 mm. The aspect ratio of walls is H/h = 2.22. The yield stress of the circular hollow sections CHS 114x3.36 is 388 N/mm^2 with an area of the section of 1167.9 mm^2. The yield stress of the CHS 88x3.36 is 380 N/mm^2 with an area of the section of 893.4 mm^2. The shear area A_v of one steel profile is estimated as half of the total steel section area. The shear area A_v of the CHS 114x3.36 and the CHS88x3.36 are thus respectively 583.9 and 446.7 mm^2. Normal longitudinal reinforcement are T12 with a yield stress of 389 N/mm^2. Transverse reinforcement are T8@150 with a yield stress of 330 N/mm^2; they provide A_{sw}=100.6mm^2 per stirrup. ρ_a ranges from 1.12 to 2.12% and $\rho_{s,tot}$ from 2.12 to 3.12%.

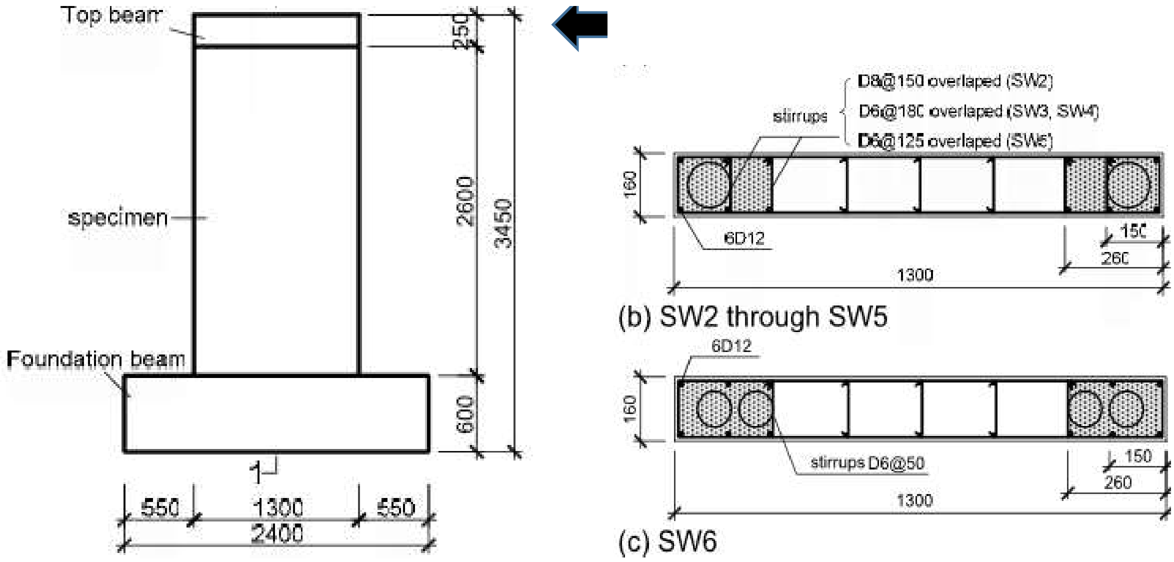

Figure 22. External dimensions and sections of the tested walls (in mm).

A constant compression force N is first applied and kept constant during the consequent cyclic application of a progressively increased horizontal force V, with force reversal. The compression force N is in the range $0.55N_{pl,Rd}$ to $0.73N_{pl,Rd}$. The force displacement curves in Figure 23 are the backbone curves of the cyclic tests.

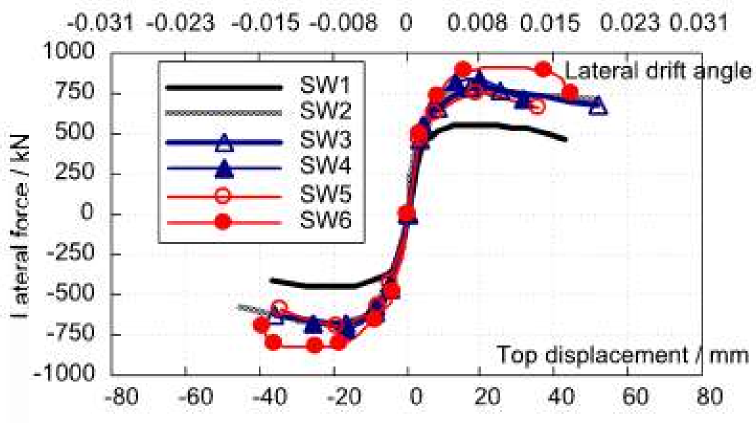

Figure 23. Envelope of experimental curves [1].

The observed failure mode is a plastic bending (cracks perpendicular to the wall axis) with a yield plateau during which diagonal shear cracks appear progressively.

9.2 Resistance to transverse shear and distribution of applied shear

Compression struts are assumed inclined at 45° and the “unit cell” height is equal to z. For specimens SW2 to SW5, z = 1170mm; for specimen SW6 is z = 1000 mm.

The elastic modulus E_c is considered the same for all specimens, i.e. $E_c = E_{cm}$ = 34000 MPa. For specimens SW2 to SW5, η = 1.11, and for specimen SW6, η = 1.21. The encased profiles are concrete filled tubes. Concrete is then likely to contribute to the shear stiffness and strength of the tubes, but to an extent which, to our knowledge, is not covered by any commonly accepted model. The choice is made here to handle the encased CFT’s as circular hollow sections (CHS) and thus to neglect any contribution of the concrete infill. In Table 8, the distribution of shear is defined for an applied shear V_{Ed} equal to the experimental yield load level.

Spec.	Encased Steel CHS Profiles	Total Shear Area A_v (mm^2)	Shear Stiffness S_{SP} (N/mm)	Shear Stiffness S_{RC} (N/mm)	$\frac{S_{SP}}{S_{SP}+S_{RC}}$	V_{Ed} (kN)	V_a (kN)	V_c (kN)
SW2	2x114x3.36	1167	81.10^3	129.10^3	0,386	601	232	369
SW3	2x114x3.36	1167	81.10^3	129.10^3	0,386	617	238	379
SW4	2x114x3.36	1167	81.10^3	129.10^3	0,386	647	250	397
SW5	2x88x3.36	934	65.10^3	129.10^3	0,335	598	200	398
SW6	4x88x3.36	1868	151.10^3	129.10^3	0,539	697	375	322

Table 8. Distribution of the applied shear in the wall and the encased profiles.

It is necessary to check if shear influences the CHS resistance to axial forces. Table 9 indicates that $V_{a,}$ is close to the sum of the plastic strength in shear $V_{pl,Rd,tot}$ of the 3 encased profiles, corresponding to a clear influence of the shear on the axial capacity of the tubes: yielding of the most stressed tube is achieved in a shear-tension interaction state. However, it is also recalled that these tests are largely entering the plastic domain, so that some strain hardening takes place, which can possibly increase the yield stress in shear by a factor of √3=1.73.

Spec	V_{Ed} kN	V_a kN	$V_{pl,Rd,tot}$ kN	$\frac{V_a}{V_{pl,Rd,tot}}$
SW2	601	232	261	0.89
SW3	617	238	261	0.91
SW4	647	250	261	0.96
SW5	598	200	209	0.96
SW6	697	375	418	0.90

Table 9. Check of shear level in encased CFT's

The average measured concrete resistance f_{cm} is given in Table 10. For design strength, the concrete resistance is: $f_{cd} = 19.1$ MPa. The effect of the applied compression force on the shear resistance resistance of the concrete has been taken into account by means of the coefficient α_{cw} of Eurocode 2[27], based on the average compression stress σ_{cp}. It can be observed in Table 10 that $V_{Rd,max} > V_{Rd,s}$ so that the ULS in shear of the RC wall corresponds to yielding of transverse reinforcement. The design resistance of walls calculated as $V_{Rd} = V_{Rd,s} + V_{pl,Rd,tot}$ provides a fair estimate of the real resistance: the ratios of calculated to experimental resistance range between 0.78 and 0.92, with an average equal to 0.84; here again, strain hardening contribute to explain why the experimental yield load is greater than V_{Rd}.

Spec.	f_{cm} MPa	$\frac{\sigma_{cp}}{f_{cd}}$	α_{cw}	$V_{Rd,max}$ kN	$V_{Rd,s}$ kN	$V_{pl,Rd,tot}$ kN	$V_{Rd} = V_{pl,Rd,tot} + V_{Rd,s}$ kN	V_y Exp kN	V_{Rd} / V_y $\frac{\text{Calcul}}{\text{Experim}}$
SW2	42.5	0.55	1.13	443	258	261	519	601	0.86
SW3	38.9	0.60	1.00	443	258	261	519	617	0.84
SW4	38.5	0.72	0.70	443	258	261	519	647	0.80
SW5	44.8	0.70	0.75	355	258	209	467	598	0.78
SW6	47.8	0.73	0.68	710	221	418	639	697	0.92

Table 10. Evaluation of steel profiles contribution to shear strength

A complementary way to check the validity of the proposed analytical expressions consists in calculating the contribution of the steel profiles to the shear resistance as the difference between the resistance measured on composite walls (specimens SW2 to SW6) and the resistance of the reference RC wall (specimen SW1) at the yield initiation and at the maximum load.

At yield : $V_{Rd,a} = V_{y,SWi} - V_{y,SW1}$

At maximum load : $V_{Rd,a} = V_{p,SWi} - V_{p,SW1}$

where $V_{y,SWi}$ is the yield resistance of wall i and $V_{p,SWi}$ is the maximum resistance of wall i

$V_{y,SW1} = 422$ kN and $V_{p,SW1} = 503$ kN

The columns (V_y - $V_{y,SW1}$) and ($V_p - V_{p,SW1}$) in Table 11 show that encased profiles contribute to the shear resistance of walls. Their contribution is properly estimated by the expression of the shear resistance of the steel profiles. There is a remarkable agreement between the experimentally measured contribution of the steel profiles to the maximum shear strength ($V_p - V_{p,SW1}$), the calculated contribution of the steel profiles to shear strength V_a and the plastic shear strength of the encased profiles $V_{pl,Rd,tot}$.

Spec.	V_{Ed} kN	V_{Ed} - $V_{y,SW1}$ kN	V_p kN	$V_p - V_{p,SW1}$ kN	$V_{pl,Rd,tot}$ kN	V_a kN
SW2	601	179	718	215	261	232
SW3	617	195	738	235	261	238
SW4	647	225	771	268	261	250
SW5	598	176	719	216	209	200
SW6	697	275	851	348	418	375

Table 11. Evaluation of steel profiles contribution to shear strength by comparison to reference RC specimen SW1.

9.3 Assessment of expressions for longitudinal shear at concrete-profiles interface

$V_{l,a}$ is calculated referring to (31) and (34) with A_{bars} of 6 diameter 12 and A_{prof} of one CHS114x3.36 in the chord zone of specimens SW2 to SW5 and 2 CHS 88x3.36 in the chord zone of specimen SW6.

As explained in 6.2, two different evaluations are made concerning the resistance to longitudinal shear at the steel concrete interface. The results in Table 12 show that design resistance to longitudinal shear is sufficient, so that shear connectors are indeed not mandatory. The second evaluation, made with probable values of average bond resistance and friction, strengthen this conclusion. Table 13.

Spec	$V_y = V_{Ed}$ kN	V_a kN	V_c kN	V_{la} kN	1 Profile perimeter mm	$V_{Rd,bond}$ kN	$V_{Rd,frict.}$ kN	$V_{Rd,total} \Leftrightarrow V_{l,a}$ kN
SW2	601	232	369	232	357	63	185	248 > 232
SW3	617	238	379	238	357	63	190	253 > 238
SW4	647	250	397	250	357	63	199	262 > 250
SW5	598	200	398	250	277	42	199	241 ≈ 250
SW6	697	375	322	232	277	83	161	244 > 232

Table 12. Evaluation of applied longitudinal shear V_{la} and comparison to the design resistance to longitudinal shear $V_{Rd,total}$ provided by bond and friction calculated with design values.

Spec	$V_y = V_{Ed}$ kN	V_a kN	$V_{l,a}$ kN	$V_{Rd,bond}$ kN	$V_{Rd,frict.}$ kN	$V_{Rd,total} \Leftrightarrow V_{la}$* kN
SW2	601	232	232	126	221	347 > 232
SW3	617	238	238	126	227	350 > 238
SW4	647	250	250	126	238	364 > 250
SW5	598	200	250	84	239	323 > 250
SW6	697	375	232	166	193	359 > 232

* with τ_R=0,6MPa and μ = 0,6

Table 13. Evaluation of applied longitudinal shear $V_{l,a}$ and comparison to the longitudinal shear resistance $V_{Rd,total}$ considering probable values of bond resistance and friction.

10 Conclusions

An analytical method for the design of walls with several encased steel profiles, or SRC walls, or steel-concrete hybrid walls is proposed. It allows checking walls subjected to a combination of applied axial force, bending and shear. In particular, the method quantifies the load sharing between concrete and encased profiles regarding the transverse shear and defines as well how to properly evaluate the longitudinal shear at the concrete-steel profiles interface; this latter information is necessary to design adequately shear connections of the profile.

The assessment of the proposed analytical method by comparison with experimental results allows drawing the following conclusions:

1) The encased profiles contribute undoubtedly to the shear stiffness and the shear resistance of hybrid walls.

2) The proposed design method provides a good estimate of the part of the applied shear that is applied to the encased steel profiles; this allows performing design checks dedicated to the interaction shear and axial force in the encased profiles.

3) The method provides a fair estimate of the longitudinal shear applied at the concrete-steel profiles interfaces for a given applied transverse shear. Tests where the calculated longitudinal shear effect approaches the longitudinal shear resistance evaluated with probable values of bond resistance τ_{Rm} and friction coefficient μ show a failure related to this mechanism. This means that the method allows correctly estimating the level of applied transverse shear leading to a failure by excessive longitudinal shear.

4) When used with design values of the bond and friction parameters taken from Eurocode 4, the method provides a safe-sided design against longitudinal shear at the concrete-steel profiles interfaces.

5) The experiments with mechanical shear connectors have shown that the summation of individual components of the resistance due to bond, friction and connectors is effective.

6) Plate connectors can be effective if the induced local compression struts activated by the load transfer from the profile to the concrete are supported in an adequate way; this can be achieved either by the appropriate orientation of the compression struts toward the wall core, or by means

of stirrups located around each profile in cases where the compression struts face an external side of the wall.

Acknowledgement

This paper was developed in the frame of the SMARTCOCO project funded by RFCS, the Research Fund for Coal and Steel of the European Commission, Research grant agreement RFSR-CT-2012-00031 Smartcoco. The companies BESIX and ArcelorMittal are also acknowledgede for their contribution and involvement in the project.

References

[1] Wallace JW, Orakcal K, Cherlin M, Sayre BL. Lateral-load behavior of shear walls with structural steel boundary columns. Proceedings of sixth ASCCS Conference on Composite and Hybrid Structures, Los Angeles, USA, 2000; 801–808.

[2] Qian.J., Jiang.Z., Ji X. Behaviour of Steel Tube-Reinforced Concrete Composite Walls Subjected to High Axial Force and Cyclic Loading. Engineering Structures 2012, 36(3):173-184

[3] Ying Zhou, Xilin Lu and Yugang Dong. Seismic Behaviour of Composite Shear Walls with Multi Encased Steel Sections. Part 1: Experiment. The Structural Design of Tall and Special Buildings, 2010; 19, 618-636. Wiley Online Library

[4] Dan, D, Fabian, A, and Stoian, V. Theoretical and experimental study on composite steel–concrete shear walls with vertical steel encased profiles, Journal of Constructional Steel Research 67. 2011; 800–813

[5] Dan, D, Fabian, A, and Stoian, V. Nonlinear behavior of composite shear walls with vertical steel encased profiles, Engineering Structures 33; 2011; 2794–2804

[6] Dan, D, Fabian, A, and Stoian, V. Numerical Investigation on the effect of axial force to the behaviour of composite steel concrete shear walls.8th International Conference on Behavior of Steel Structures in Seismic Areas Shanghai, China; 2015; July 1-3

[7] Ji.X., Sun, Y, Qian.J., Lu, X. Seismic Behaviour and modelling of steel reinforced concrete (SRC) walls. Earthquake Engng. Struct.Dyn.; 2015; 44:975-972

[8] AISC Standard 341–10. Seismic provisions for structural steel buildings. American Institute of Steel Construction: Chicago, 2010. One East Wacker Drive, Suite 700, Chicago, Illinois 60601-1802

[9] CEN. Eurocode 8: Design Provisions for Earthquake Resistance-Part 1: General Rules, Seismic Actions and Rules for Buildings. European Committee for Standardization: Brussels, 2004.

[10] JGJ 3–2010. CMC. Technical specification for concrete structures of tall building (JGJ 3–2010). China Ministry of Construction: Beijing, 2011.

[11] Vulcano A, Bertero VV, Colotti V. Analytical modeling of R/C structural walls. Proceedings, 9th World Conference on Earthquake Engineering 1988; 6:41–46.

[12] Orakcal K, Wallace JW, Conte JP. Flexural modeling of reinforced concrete walls-model attributes. ACI Structural Journal 2004; 103(2):196–206.

[13] PEER/ATC. Modeling and acceptance criteria for seismic design and analysis of tall buildings. PEER/ATC 72-1 Report, Applied Technology Council, Redwood City, CA, October 2010.

[14] Miao Z, Ye L, Guan H, Lu X. Evaluation of modal and traditional pushover analyses in frame-shear-wall structures. Advances in Structural Engineering 2011; 14(5):815–836.

[15] Lu X, Lu X, Guan H, Ye L. Collapse simulation of reinforced concrete high-rise building induced by extreme earthquakes. Earthquake Engineering and Structural Dynamics 2013; 42(5):705–723.

[16] Degee H, Plumier A, Mihaylov B, Dragan D, Bogdan T, Popa N, De Bel J-M, Mengeot P, Hjiaj M, Nguyen QH, Somja H, Elghazouli A, Bompa D, Smart Composite Components – Concrete Structures Reinforced by Steel Profiles “SmartCoCo”, 2016 (to be published)

[17] Eurocode 4 (2004), EN 1994-1-1 Design of composite steel and concrete structures, Part 1.1– General Rules for buildings;2004; European Committee for Standardizations, Brussels.

[18] AISC 360-10 Specification for Structural Steel Buildings, 2010; American Institute for Steel Construction, One East Wacker Drive, Suite 700, Chicago, Illinois 60601-1802

[19] Bogdan T, Plumier A, Degee H, A proposal for the design of concrete sections reinforced by multiple encased rolled steel sections, Eurosteel Conference 2014, September 10-12, Naples, Italy

[20] Bogdan T, Popa N, Smartcoco Project Deliverable 5.1.Cross checks between HBCol and Finite Element Models in SAFIR, 2016, ArcelorMittal Global R&D Report. To be published.

[21] Plumier A, Smartcoco Project Deliverable 2.2. Generic Design Approach, 2016, Plumiecs Report. To be published.

[21] Plumier A, Bogdan T, Degee H, Design of columns with several encased steel profiles for combined compression and bending. Internal Report University of Liege – ArcelorMittal. 2013. Available on request.

[22] Plumier A, Bogdan T, Degee H, Design for shear of columns with several encased steel profiles. Internal Report University of Liege – ArcelorMittal. 2013. Available on request.

[24] Mörsch, E., "Der Eisenbetonbau, seine Theorie and Anwendung" (Reinforced Concrete, Theory and Application), Verlag Konrad Wittwer, Stuttgart, 1912.

[25] Dan Dragan. Report on Smartcoco Project Deliverable D6-1 Part 1 – Tests at ULg; 2016; to be published.

[26] Nguyen Quang Huy, 2016. Report on Smartcoco Project Deliverable D6-1 Part 2 – Tests at INSA Rennes; 2016; to be published.

[27] Eurocode 2 (2004), EN 1992-1-1 "Design of concrete structures, Part 1.1 – General Rules for buildings";2004; European Committee for Standardizations, Brussels.

[28] TML Strain Gauges. Download at: https://www.tml.jp/e/download/catalogdownload.html

[29] Eurocode 3 (2004), EN 1993-1-1 "Design of steel structures, Part 1.1 – General Rules and rules for buildings";2004; European Committee for Standardizations, Brussels.

[30] Building Code Requirements for Structural Concrete (ACI 318-14), September 2014, An ACI Standard, ISBN: 978-0-87031-930-3